Polymer deformation in Brownian ratchets: Theory and molecular dynamics simulations

Martin Kenward*
Department of Chemical Engineering and Materials Science, University of Minnesota, 421 Washington Avenue SE, Minneapolis, Minnesota 55455, USA

Gary W. Slater†
Department of Physics, University of Ottawa, 150 Louis-Pasteur, Ottawa, Ontario, Canada K1N 6N5
(Received 27 August 2008; published 25 November 2008)

We examine polymers in the presence of an applied asymmetric sawtooth (ratchet) potential which is periodically switched on and off, using molecular dynamics (MD) simulations with an explicit Lennard-Jones solvent. We show that the distribution of the center of mass for a polymer in a ratchet is relatively wide for potential well depths U_0 on the order of several k_BT. The application of the ratchet potential also deforms the polymer chains. With increasing U_0 the Flory exponent varies from that for a free three-dimensional (3D) chain, $\nu=3/5$ ($U_0=0$), to that corresponding to a 2D compressed (pancake-shaped) polymer with a value of $\nu=3/4$ for moderate U_0. This has the added effect of decreasing a polymer's diffusion coefficient from its 3D value D_{3D} to that of a pancaked-shaped polymer moving parallel to its minor axis D_{2D}. The result is that a polymer then has a time-dependent diffusion coefficient $D(t)$ during the ratchet off time. We further show that this suggests a different method to operate a ratchet, where the off time of the ratchet, t_{off}, is defined in terms of the relaxation time of the polymer, τ_R. We also derive a modified version of the Bader ratchet model [Bader *et al.*, Proc. Natl. Acad. Sci. U.S.A. **96**, 13165 (1999)] which accounts for this deformation and we present a simple expression to describe the time dependent diffusion coefficient $D(t)$. Using this model we then illustrate that polymer deformation can be used to modulate polymer migration in a ratchet potential.

DOI: 10.1103/PhysRevE.78.051806 PACS number(s): 61.41.+e, 83.10.Mj, 82.20.Wt

I. INTRODUCTION

The environment in which biological macromolecules are found is a tempestuous one. The constant bombardment (i.e., Brownian motion) experienced by entities at the molecular scale (nanometers) is the source of diffusion and is directly related to molecular transport. It is a seemingly impossible task to generate deterministic motion against the forces to which a molecule is subject at these length scales (with typical energies on the order of k_BT). Borrowing an analogy from Bier, directed motion at the molecular level is akin to humans attempting to swim in molasses [2]. In spite of this, molecular processes work almost unimaginably well.

A key element of this success is a *molecular toolkit* which has evolved to inherently use diffusion in transport processes as opposed to it being a detriment. This is counterintuitive as diffusion is sometimes the bane of directed transport, often as a result of myopic attempts to scale down macroscopic manipulation techniques, for example for use in microfluidic applications. Instead, diffusion plays an enormously important role in transport and we are only now beginning to fully appreciate and take advantage of its consequences [3–8].

The crucial question is then: How does a system (e.g., a piece of cellular machinery) extract useful work from the random fluctuations affecting a diffusing molecule? The second law of thermodynamics strictly forbids a periodic system at thermal equilibrium from performing any work. Therefore, in order to extract work the general *modus operandi* is to drive the system out of thermal equilibrium and to break its spatial inversion symmetry, although other operational modes are possible [4]. These techniques are referred to as ratcheting effects and the mechanism itself as a ratchet. The classic illustrative example of this phenomenon is the Feynman-Smoluchowski ratchet, consisting of a ratchet and pawl system at thermal equilibrium; no directed motion is then possible [9–11]. The variant of this system in which the ratchet and pawl are thermally isolated from one another at different temperatures (broken thermal equilibrium) is able to perform useful work. The review of Reimann [4] gives the detailed historical development of ratchets.

In this paper we focus on the use of broken spatial inversion symmetry, manifested by the application of an asymmetric spatially periodic potential, to generate directed transport. Numerous analogs of this method exist in biological systems, including the pumping mechanism in ion channels [7] and the movement of myosin along an actin filament [7]. These ratchets operate in one of two modes: a flashing mode (in which the ratchet is periodically switched on and off) [4–6,12], or a tilted mode in which an external force is applied in addition to the periodic switching of the ratchet [2,4]. We restrict our work to a discussion of flashing ratchets.

Within the rapidly growing fields of micro- and nanofluidics, methods that can effectively (and efficiently) manipulate material in environments where Brownian motion has non-negligible effects are increasingly important [7]. Ratchets (in their various forms) are one set of techniques which are at the forefront of this technological revolution [7]. A particular application, the manipulation of unfolded biological macromolecules (DNA for example), whether it be for

*mkenward@cems.umn.edu
†Corresponding author; gslater@uottawa.ca

separation purposes or purely transport methodologies, is the intrinsic motivation for our work.

In this paper we carry out a systematic examination of the behavior of polymers in (flashing) asymmetric sawtooth (ratchet) potentials using molecular dynamics simulations in which we explicitly include solvent particles and thus a self-consistent representation of hydrodynamics. We restrict our examination to regimes where the width of the ratchet is on the order of the polymer radius of gyration, R_g.

We provide an examination of the role of polymer deformation induced by the application of the ratchet. This deformation alters the equilibrium steady state friction coefficient of the molecules, ξ, and consequently the diffusion coefficient D, both of which are functions of the effective size and shape of the molecules. This deformation most certainly affects ratchet operation; however, it has not been included in current ratchet models. Downton *et al.* [5] and Craig *et al.* [6] have examined a number of aspects of polymer dynamics in ratchets using Brownian dynamics simulations (with no hydrodynamics), and in particular they have examined the role of the internal degrees of freedom of the polymer chains in the transport of polymers in ratchets and the effects of mechanical coupling of objects in ratchets. An explicit solvent allows us to directly examine the effects of deformation (for hydrodynamically impermeable coils) and associated effects on polymer dynamics in ratchets resulting from hydrodynamic interactions.

II. SIMULATION MODEL

We use a similar molecular dynamics (MD) model as described previously [13,14] and found in numerous other publications [15]. The model is a variant of the classic Kremer-Grest model for coarse-grained polymer systems. We have two constituent components in the system. The first are *soft* fluid particles, which interact solely via the repulsive part of the Lennard-Jones (LJ) potential given by

$$V_{\mathrm{LJ}}(r) = \begin{cases} 4\epsilon\left[\left(\frac{\sigma}{r}\right)^{12} - \left(\frac{\sigma}{r}\right)^{6}\right] + \epsilon, & r \leqslant r_c, \\ 0, & r \geqslant r_c, \end{cases} \tag{1}$$

where σ and ϵ are the length and energy scales, r is the center-to-center distance between two beads, and $r_c = \sqrt[6]{2}\sigma$ is the position of the minimum in the Lennard-Jones potential and corresponds to the cutoff for calculating forces [15].

The second component in our systems consists of polymers constructed via a series of contiguous LJ particles which are effectively *bonded* together using the finitely extensible nonlinear elastic (FENE) potential [15]

$$V_{\mathrm{bond}}(r) = -\frac{\kappa}{2}R_0^2 \ln\left[1 - \left(\frac{r}{R_0}\right)^2\right], \tag{2}$$

where R_0 is the upper bound on the bond distance and κ is an effective spring constant. The linear polymers are modeled as N_p Lennard-Jones beads connected via $N_p - 1$ FENE bonds. The use of the FENE potential ensures that the chains have a finite range of extensions. We use the standard values $\kappa = 30.0\epsilon/\sigma^2$ and $R_0 = 1.5\sigma$ [15,16]. The temperature in all of the simulations is chosen to be $k_B T = 1$.

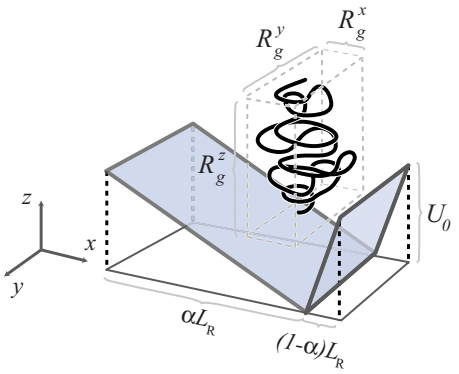

FIG. 1. (Color online) Schematic illustration of a polymer confined within an asymmetric sawtooth potential with an asymmetry parameter $0.5 \leqslant \alpha \leqslant 1$. The length of the ratchet unit cell is L_R. The polymer is compressed in the x direction as a result of the application of the ratchet potential of depth U_0.

Our simulations can have on the order of $10^4 \leqslant N_s \leqslant 10^5$ solvent particles. The reduced density of the system is set at a value of $\rho = 0.85\sigma^{-3}$ [13,15]. The viscosity of the solvent (as calculated previously) is $\eta = 2.25 \pm 0.05$ and the corresponding single-bead friction coefficient is $\xi_s = 16.2 \pm 0.2$ [13] in MD units.

The equations of motion for the system are written in reduced units and integration is carried out using the standard velocity Verlet algorithm [15,17] with an integration time step of $\delta t = 0.01$. More thorough descriptions of the entire MD simulation method can be found throughout the literature [15,17].

In order to control to the temperature in our systems we use a dissipative particle dynamics (DPD) thermostat. The crux of the DPD method involves damping differences in particle pair velocities. The DPD thermostat has been shown to preserve hydrodynamic interactions and is becoming the method of choice for many practitioners of MD [18]. Detailed descriptions of the DPD method and its derivation abound in the literature [19]. The time step we use in our simulations provides robust thermostatting and we checked that our results presented here are effectively invariant to small changes in δt.

A. Ratchet potential

We use an asymmetric sawtooth potential for our ratchet (see Fig. 1), which is given by the following piecewise continuous function:

$$\frac{U_R(x')}{k_B T} = U_0 \times \begin{cases} \dfrac{\alpha L_R - x'}{\alpha L_R}, & 0 \leqslant x' < \alpha L_R, \\ \dfrac{\alpha L_R + x'}{(1-\alpha)L_R}, & \alpha L_R \leqslant x' \leqslant L_R, \end{cases} \tag{3}$$

where L_R is the ratchet unit cell width and $x' = x \bmod L_R$ is the position inside the potential. The parameter α is the effective asymmetry parameter of the ratchet ($\alpha = 0.5$ implies a symmetric potential). The depth of the well is U_0 and is kept in the range $U_0 \in [0, 10]$ which corresponds to the normal op-

erational range for experimental ratchet systems [1,5]. Figure 1 shows a schematic depiction of a polymer confined in this ratchet potential. The polymer is shown in a compressed pancake-shaped state and the effective dimensions of the chain are shown (discussed later).

The ratchet potential is operated in a binary mode and thus it is either on or off. The corresponding on and off times are t_{on} and t_{off}, respectively. Values of $t_{on}=0$ and $t_{off}=0$ provide purely off and purely on states of the ratchet. Variations in α, U_0, t_{on}, and t_{off} alter the dynamics and conformations of particles and molecules in the presence of the ratchet and can induce net transport [4].

III. POLYMER DEFORMATION IN ASYMMETRIC SAWTOOTH POTENTIALS

In this section we examine the effects of confining polymer chains within the asymmetric sawtooth potential described by Eq. (3) and Fig. 1. The application of this potential has a number of consequences, most notably the deformation of the polymer chain. The degree to which the chains are deformed (relative to free chains) is dictated by U_0 and α. Larger U_0 yields larger deformation. In the limit of $U_0 \to \infty$ we obtain two-dimensional (2D) pancake-shaped polymers in the y-z plane and the chain Flory exponent is $\nu_{2D}=3/4$ [20,21]. Conversely, in the absence of the potential (i.e., $U_0=0$) the Flory exponent is $\nu_{3D}=3/5$ [20,21]. Both ν_{3D} and ν_{2D} are strictly valid in the large-chain limit (i.e., as $N_p \to \infty$). In practice, both the potential and resulting deformation are finite with $\nu \in [\nu_{2D}, \nu_{3D}]$. Larger U_0 also leads to sharper localization of the chains.

The asymmetry parameter of the potential, α, determines the relative position in the ratchet at which polymers localize. Defining $\rho_{c.m.}(x)$ as the normalized probability distribution of the polymer center of mass, the parameter α controls whether $\rho_{c.m.}(x)$ is symmetric ($\alpha=0.5$) or asymmetric ($0.5 < \alpha \leqslant 1$). The combined variation of α and U_0 thus modulates the position of the maximum in $\rho_{c.m.}(x)$ and its sharpness and symmetry.

We use several metrics to gauge the effects of α and U_0 on the polymer chains. The first is the averaged squared end-to-end distance:

$$\langle R_e^2 \rangle \equiv \langle |\vec{r}_1 - \vec{r}_{N_p}|^2 \rangle \tag{4}$$

where $|\vec{r}_1 - \vec{r}_{N_p}|$ is the norm of the vector connecting the two terminal monomers of the chain and $\langle \cdots \rangle$ denotes a temporal average. For $U_0=0$ the end-to-end distance is predicted to scale as $R_e \propto N_p^{\nu_{3D}}$, for large N_p [20].

The other metrics of chain deformation are obtained from the gyration tensor given by

$$\mathsf{R}^2 = \begin{pmatrix} R_{11}^2 & R_{12}^2 & R_{13}^2 \\ R_{21}^2 & R_{22}^2 & R_{23}^2 \\ R_{31}^2 & R_{32}^2 & R_{33}^2 \end{pmatrix}. \tag{5}$$

The elements of this tensor are

$$R_{ij}^2 \equiv \frac{1}{N_p} \sum_{k=1}^{N_p} (x_{i,k} - x_{i,c.m.})(x_{j,k} - x_{j,c.m.}), \tag{6}$$

where $x_{i,k}$ and $x_{i,c.m.}$ are the position of the kth monomer and the center of mass, respectively (direction $i=1,2,3$ implies x,y,z). The trace of R^2 is the squared radius of gyration:

$$R_g^2 \equiv \mathrm{Tr}\mathsf{R}^2 = R_{11}^2 + R_{22}^2 + R_{33}^2. \tag{7}$$

Equation (7) is equivalent to the standard expression for the radius of gyration,

$$R_g^2 \equiv \left\langle \frac{1}{N_p} \sum_{i=1}^{N_p} |\vec{r}_i - \vec{r}_{c.m.}|^2 \right\rangle, \tag{8}$$

where $\vec{r}_i - \vec{r}_{c.m.}$ is the vector connecting the ith monomer and the molecule's center of mass $\vec{r}_{c.m.}$, which is defined by

$$\vec{r}_{c.m.} = \frac{1}{N_p} \sum_{i=1}^{N_p} \vec{r}_i. \tag{9}$$

The radius of gyration R_g gives a measure of effective polymer size and unlike R_e it is equally useful for circular and branched polymers. For $U_0=0$, the radius of gyration also scales as $R_g \propto N_p^{\nu_{3D}}$ ($N_p \gg 1$) [20].

Although R_g and R_e do give a measure of effective polymer size there is a caveat: neither R_g nor R_e yields information about the instantaneous conformational anisotropy (or shape) of the molecules. The molecules' relative anisotropy is characterized using their principal radii of gyration. They are the solutions of the characteristic equation $\det|\mathsf{R}^2 - \lambda \mathsf{I}| = 0$ for the eigenvalues, $\lambda = R_{x'}^2, R_{y'}^2, R_{z'}^2$, (such that $R_{x'}^2 \leqslant R_{y'}^2 \leqslant R_{z'}^2$) [20]. The three principal radii of gyration are given by the average of these eigenvalues, $R_g^\beta = \langle R_\beta^2 \rangle^{1/2}$ ($\beta = x', y', z'$). They give us an indicator of the anisotropy (and deformation) of the molecules. In the $U_0 \to \infty$ limit, the minor axis is aligned in the x direction and the two major axes are in the y-z plane.

We used these metrics to determine the size and anisotropy of molecules in our MD simulations resulting from the application of the ratchet potentials We do not explicitly explore the orientations of the associated eigenvectors of the molecules here. The simulation cell used for these calculations has dimensions $L_x \times L_y \times L_z$ ($L_\beta = 46.449\sigma$ or roughly 44 LJ beads wide). The width of the ratchet is $L_R = 11.612\sigma$, with four potential wells per simulation cell. Systems are initially allowed to relax for a minimum of 100 000 time steps. The potential is then turned on and the system is allowed to relax for an additional 100 000 MD time steps followed by data collection for 2×10^7 MD time steps.

A. MD results for deformation (nonflashing potential)

We begin by examining the chain metrics described above for $N_p \in [3,41]$ and for potentials purely in the on state with well depths of $U_0=0,2,4,8$. For the $U_0=0$ case, we have a free chain (a self-avoiding random coil in the large-N_p limit). Figure 2 shows a log-log plot of $R_g^{x'}$, $R_g^{y'}$, and $R_g^{z'}$ as a function of N_p. The inset of Fig. 2 shows a semilogarithmic plot

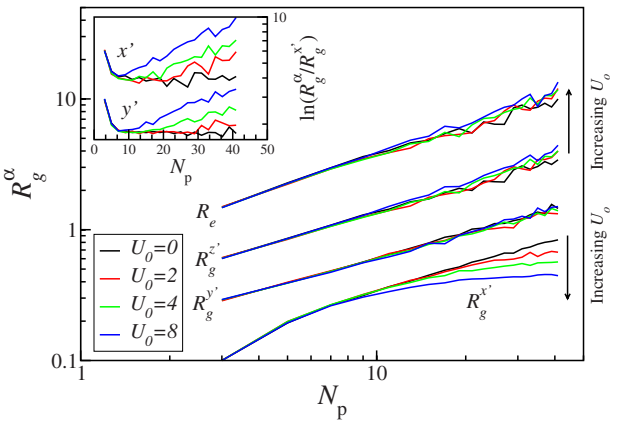

FIG. 2. (Color online) Log-log plot of the three principal radii of gyration $R_g^{x'}$, $R_g^{y'}$, and $R_g^{z'}$ and the end-to-end distance R_e as a function of N_p for well depths $U_0 \in [0,8]$ with $\alpha=0.8$. Inset: Semilogarithmic plot of the ratios $R_g^{y'}/R_g^{x'}$ and $R_g^{z'}/R_g^{x'}$ as functions of N_p, illustrating the effective asymmetry of the chains as measured in the principal axis system. The radius of gyration is not shown but is simply obtained from $R_g^2=(R_g^{x'})^2+(R_g^{y'})^2+(R_g^{z'})^2$. As U_0 is increased the polymer is compressed by the asymmetric sawtooth potential. For large N_p, $R_g^{x'}$ decreases with increasing U_0 and becomes a weak function of N_p.

of the ratio of $R_g^{z'}/R_g^{x'}$ and $R_g^{y'}/R_g^{x'}$ as a function of N_p and thus gives an effective measure of the molecular asymmetry. As expected, in the $U_0=0$ case molecules appear anisotropic as measured in the principal axis system, as evidenced in Fig. 2. From Fig. 2 it would appear that for $U_0>0$ and $N_p \leqslant 10$ the chains are also essentially undeformed relative to the free chains and most likely the molecules are simply being rotated into the plane of the ratchet potential. However, the molecules are anisotropic as the inset of Fig. 2 clearly illustrates. For the short chains the degree of anisotropy is about the same as that for the free chains. However, for $N_p>10$ the molecules have increased anisotropy as a result of a stronger competition between the ratchet potential and the chain entropy (both conformational and rotational). For large U_0, $R_g^{x'}$ begins to saturate with N_p and the asymmetry of the chain is an increasing function of U_0. Larger U_0 would further constrain the polymers to the y-z plane. Clearly, from Fig. 2, $R_g^{x'}$ does not vary as a power law with N_p. As we increase U_0 the plateau value of $R_g^{x'}$ (for large N_p) decreases corresponding to the increasing confinement of the chain.

We have also calculated an effective Flory scaling ν as a function of U_0 (for R_g, R_e, $R_g^{y'}$, and $R_g^{z'}$). The values of ν are extracted from a linear regression of the data in Fig. 2. The calculated values of ν (for $N_p>20$) are shown in Fig. 3 as a function of U_0. Also shown are the asymptotic values for ν [$U_0 \to \infty$ ($\nu=\nu_{2D}$) and $U_0 \to 0$ ($\nu=\nu_{3D}$)] for self-avoiding chains [20]. We see that for all measures of the chain size, ν plateaus with increasing U_0 as the chains are progressively more confined in the plane of the ratchet potential. For $U_0=0$ the calculated values of ν are slightly higher than ν_{3D}. Our relatively short chains appear somewhat stiff and skew ν toward a slightly higher value.

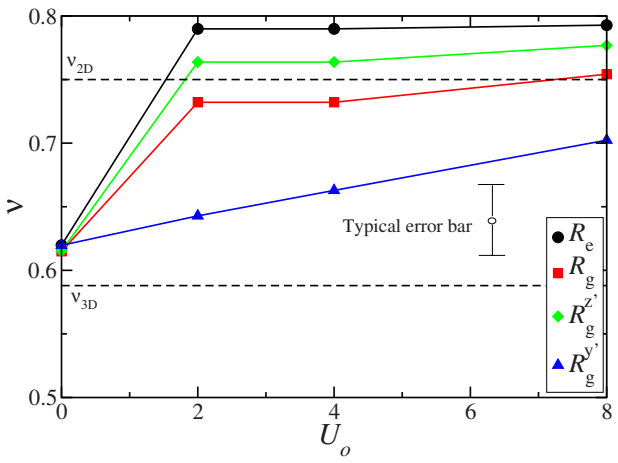

FIG. 3. (Color online) Flory exponent ν as a function of U_0, calculated for chains larger than $N_p>20$ for the measures of chain size given by R_g, R_e, $R_g^{y'}$ and $R_g^{z'}$. For $U_0=0$ the polymers are free chains, while as U_0 increases the chains are squashed in the y-z plane. This illustrates the transition from three-dimensional random coils to two-dimensional pancaked chains. Also shown is a typical error bar for the values of ν.

B. Polymer localization (nonflashing potential)

We examine the localization of the polymer chains by directly calculating $\rho_{\text{c.m.}}(x)$ (the distribution of the polymer center of mass) from our simulations. Figure 4 shows $\rho_{\text{c.m.}}(x)$ for $N_p=5$ and 41 as a function of the well depth U_0 and $\alpha=0.90$. For $U_0=0$, $\rho_{\text{c.m.}}(x)$ is obviously a flat distribution with no spatial localization (not shown). For small U_0, the chains become localized to the minimum in the potential; however, $\rho_{\text{c.m.}}(x)$ is still rather broad. The distribution $\rho_{\text{c.m.}}(x)$ contains other information.

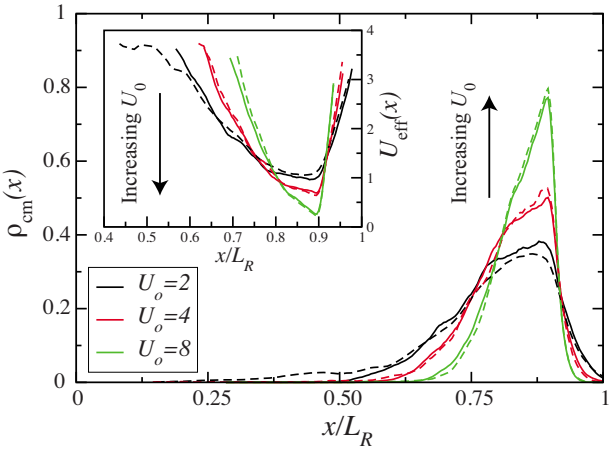

FIG. 4. (Color online) Probability distribution for the position of the polymer center of mass, $\rho_{\text{c.m.}}(x)$, for $U_0=2,4,8$ for $N_p=5$ and 41 (corresponding to dashed and solid lines, respectively). The molecules $N_p=5$ and 41 have radii of gyration of $R_g \simeq 0.95$ and 4.2, respectively; both chains are less than half the width of the ratchet unit cell. Inset: Semilogarithmic plot of $U_{\text{eff}} \equiv -\ln[\rho_{\text{c.m.}}(x)]$ as a function of x and thus the effective potential the polymer would experience if it were treated as a pointlike particle. As U_0 increases U_{eff} tends toward the actual shape of the ratchet potential, as expected.

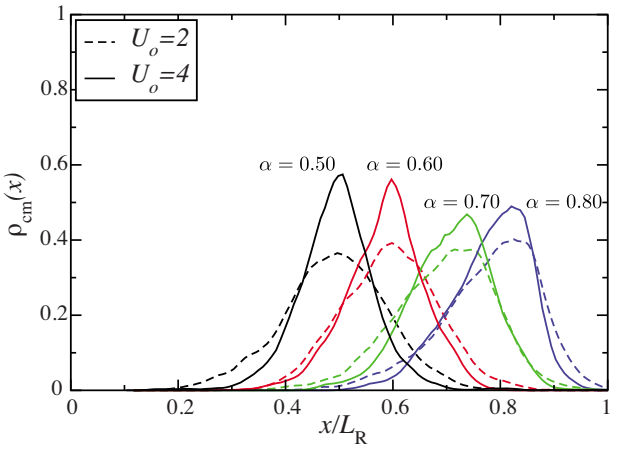

FIG. 5. (Color online) Probability distribution for the position of the polymer center of mass, $\rho_{\text{c.m.}}(x)$, as a function of α for well depths of $U_0=2,4$ and a chain length of $N_p=41$. For a purely symmetric potential $\alpha=0.5$, the resulting $\rho_{\text{c.m.}}(x)$ is also symmetric. As α is increased, $\rho_{\text{c.m.}}(x)$ tends toward a skewed distribution, with a peak position corresponding closely to the minimum in the ratchet potential.

Treating the polymer as an equivalent pointlike particle, with a position corresponding to its center of mass, we can write $\rho_{\text{c.m.}}(x)$ as

$$\rho_{\text{c.m.}}(x) \propto \exp\left(-\frac{U_{\text{eff}}(x)}{k_B T}\right), \tag{10}$$

where $U_{\text{eff}}(x)$ is the effective potential experienced by the polymer [this is shown for our particular example in Fig. 4 (inset)]. For large U_0 the effective potential tends toward the ratchet potential [i.e., $U_{\text{eff}}(x) \to U_R(x)$] as the latter greatly outweighs any other factors. It is also remarkable to note that the distributions are not significantly differently for two chains with quite different lengths $N_p=5$ and 41. In order for our ensuing analysis to hold we need to make sure that the effective size of the molecules is smaller than the ratchet potential; the molecules $N_p=5$ and 41 have radii of gyration of $R_g \simeq 0.95$ and 4.2, respectively, and both molecules easily fit in a single ratchet unit cell (i.e., $R_g < L_R$). The parameter α controls the asymmetry of the ratchet potential. For $\alpha=0.5$ the potential and the resulting center of mass distribution are symmetric. Symmetric flashing potentials are unable to induce net transport [4]. As $\alpha > 0.5$ the distribution $\rho_{\text{c.m.}}(x)$ changes from being symmetric to asymmetric.

We examine the effect of the potential asymmetry by varying $\alpha \in [0.5,1]$ ($\alpha=1$ is ill defined in our context). The range $\alpha \in [0,0.5]$ simply reverses the direction of the ratchet if it were flashed off and on. Figure 5 shows $\rho_{\text{c.m.}}(x)$ for a polymer with $N_p=41$ (both $U_0=2$ and $U_0=4$) as a function of α. For $\alpha=0.5$ both the ratchet potential $U_R(x)$ [defined in Eq. (3)] and $\rho_{\text{c.m.}}(x)$ are symmetric. As α is increased the peak in $\rho_{\text{c.m.}}(x)$ shifts to the right following the shift in minimum of the potential.

To summarize, an increase in U_0 both increases the relative deformation of the molecules and leads to a sharper distribution $\rho_{\text{c.m.}}(x)$, although the distribution always has a finite width. On the other hand α primarily controls the position of the peak in $\rho_{\text{c.m.}}(x)$ and the skewness of $\rho_{\text{c.m.}}(x)$. It should be noted that this is an oversimplification, and the variation of U_0 and α has coupled effects; however, the discussion above provides a good first-order description of their effects. Variations in U_0 also control the spatial localization of the polymers. It is usually assumed that (for large t_{on}) chains are fully localized to the potential minima [i.e., $\rho_{\text{c.m.}}(x)=\delta(x-\alpha L_R)$], where $\rho_{\text{c.m.}}(x)$ is the probability distribution of the center of mass of the polymer, or that the width of the ratchet is much larger than the width of $\rho_{\text{c.m.}}(x)$ [1,4]. Of course, as $U_0 \to \infty$ the distribution $\rho_{\text{c.m.}}(x) \to \delta(x-\alpha L_R)$. The assumption of complete localization greatly simplifies ratchet models; however, it is not necessarily realistic. Essentially, one normally assumes that the polymer behaves as an equivalent pointlike particle, localized to the minimum in the potential.

IV. POLYMER DEFORMATION VERSUS DIFFUSION

As illustrated in Sec. III B, if a polymer is treated as a pointlike particle (with position corresponding to its center of mass) the assumption of complete localization to the ratchet minima is not correct. Nonetheless, this assumption is made in most ratchet models. In other words, the polymer center of mass is assumed to be a δ function distributed as $\rho_{\text{c.m.}}(x) \simeq \delta(x-x')$, where x' is the position of the ratchet minimum. While this is reasonable for ratchets which are wide compared to the width of the polymer center of mass distribution and sufficiently deep ($U_0 \gg 1$ [1]), it is not strictly valid. However, it does greatly simplify analysis. In the calculations that follow we assume (for simplicity) that polymers are completely localized. The extension to finite-width polymer distributions is relatively straightforward.

Working with the ansatz that $\rho_{\text{c.m.}}(x)=\delta(x-x')$, the polymer center of mass distribution will evolve as

$$P(x,t) = \frac{1}{\sqrt{4\pi D t}} \exp\left(-\frac{(x-x')^2}{4Dt}\right), \tag{11}$$

where D is the free diffusion coefficient of the polymer. Normally, at fixed chain length N_p, the diffusion coefficient D is modeled as invariant to the application of the ratchet potential. In other words, the chains are assumed to be undeformed during the entire ratcheting sequence and the diffusion coefficient is assumed constant.

Even for $U_0 \simeq 10$ the diffusion coefficient undergoes a transition from $D=D_{3D}$ to the 2D (pancake) diffusion coefficient $D=D_{2D}$. It should be noted that D_{2D} refers to the diffusion coefficient of the polymer parallel to its minor axis and thus perpendicular to the plane of the ratchet potential. One could alternatively define two separate diffusion coefficients $D_{2D}^{\parallel}$ and $D_{2D}^{\perp}$ to denote the diffusion coefficients that are parallel to the minor and major axes of the polymer, respectively. For simplicity of notation we use $D_{2D}=D_{2D}^{\parallel}$ throughout. The transition from a 3D coil to a 2D pancake is illustrated by the change in the scaling of the polymer chain from ν_{3D} to ν_{2D} with increasing U_0 in Sec. III. Consequently, two deficits exist in most ratchet models: the assumption of

complete localization and the lack of an accurate description of the polymer diffusion coefficients for moderate to large U_0. We will focus on adding the second-order correction to existing ratchet models for the latter point.

The diffusion coefficient D_{3D} of a freely diffusing (undeformed and hydrodynamically impermeable) polymer is

$$D_{3D} \sim \frac{k_B T}{\eta R_H} \propto N_p^{-3/5}, \tag{12}$$

where $R_H \simeq \frac{2}{3} R_g^{3D}$ is the hydrodynamic radius of the polymer [21]. The diffusion coefficient of a pancake-shaped (2D) polymer moving face-on to its minor axis is

$$D_{2D} \sim \frac{k_B T}{\eta R_g^{2D}} \propto N_p^{-3/4}, \tag{13}$$

where R_g^{2D} is the in-plane radius of gyration of the 2D disk-like polymer [22]. In fact, maximizing the differences between $D_{2D}^{\parallel}$ for different polymers is critical for maximizing the efficiency of the ratchet. The diffusion of the polymers during the off phase of the ratchet in part controls the separation efficiency of the ratchet [6]

It is easily shown using a scaling argument that, beyond a few monomers, $D_{2D} < D_{3D}$. As a result, polymer diffusion (during the off phase of the ratchet) is initially inhibited by the pancaking effect until the polymer has relaxed. In principle this idea should be valid for chains that are not random coils due to the inherent anisotropy of polymers. Similar calculations could be applied to stiff polymers as well.

As a result, a pancake-shaped polymer diffusion coefficient will initially be D_{2D} immediately after the potential is switched off. The polymer will then diffuse and also its diffusion coefficient will relax back to D_{3D}. This relaxation will occur in a similar way to that of the end-to-end vector [21] and we use a simple interpolation scheme to model the transition from D_{2D} to D_{3D} as

$$D(t) = D_{2D} \exp\left(-\frac{t}{\tau}\right) + D_{3D}\left[1 - \exp\left(-\frac{t}{\tau}\right)\right], \tag{14}$$

where τ is a characteristic relaxation time scale for the polymer. A natural time scale over which the polymer will relax is its end-to-end vector relaxation time τ_R and we assume that $\tau \simeq \tau_R$. More robust methods exist for obtaining $D(t)$; however, Eq. (14) both has a simple functional form and allows an analytical result in the following discussion. The relaxation time [21] is given by the scaling law

$$\tau_R \simeq \frac{(R_g^{3D})^2}{6 D_{3D}}. \tag{15}$$

The polymer relaxes as it diffuses over a distance on the order its of own radius, R_g^{3D}.

An inhibited diffusion coefficient has two consequences for operational modes of a ratchet. First, polymer diffusion is slowed for off times $t_{off} < \tau_R$ and, second, if the ratchet is subsequently switched on before the polymer has relaxed it will be deformed during the on phase of the ratchet, thus affecting polymer localization.

The *classic* minimum operational ratchet off time for an undeformed polymer with diffusion coefficient D_{3D} is

$$t_{off}^{opt} = \frac{r_{eff}^2}{2 D_{3D}}, \tag{16}$$

where $r_{eff} = (1-\alpha) L_R$ is the short side distance in the ratchet, i.e., the distance the polymer must diffuse to traverse to the next ratchet cell. Equation (16) thus assumes no polymer deformation. In the case of a pancake-shaped polymer (i.e., a polymer with diffusion coefficient D_{2D}), Eq. (16) underestimates the actual minimum time required for the polymer to diffuse one well in the ratchet since $D_{2D} < D_{3D}$.

A. Modified Bader ratchet model

We now provide a derivation of a modified ratchet model discussed by Bader *et al.* [1] which includes the effects of polymer deformation and an associated time dependent diffusion coefficient. We solve the diffusion equation

$$\frac{\partial P(x,t)}{\partial t} = 2 D(t) \frac{\partial^2 P(x,t)}{\partial x^2} \tag{17}$$

for polymers that have time-dependent diffusion coefficients given by $D(t)$. To solve for $P(x,t)$, we rewrite Eq. (17) as

$$\frac{\partial P(x,\sigma^2(t))}{\partial \sigma^2(t)} = \frac{\partial^2 P(x,\sigma^2(t))}{\partial x^2}, \tag{18}$$

where

$$\sigma^2(t) = 2 \int_0^t D(t') dt'. \tag{19}$$

Our expression for $D(t)$ [in Eq. (14)] allows an analytical calculation of $\sigma^2(t)$ and is given by

$$\sigma^2(t) = 2 D_{3D} t - 2 \tau_R (D_{3D} - D_{2D})(1 - e^{-t/\tau_R}). \tag{20}$$

The probability distribution for the polymer is then

$$P(x,t) = \frac{1}{\sqrt{2\pi\sigma^2(t)}} \exp\left(-\frac{x^2}{2\sigma^2(t)}\right) \tag{21}$$

with $\sigma^2(t)$ given by Eq. (20). In the case that $D_{3D} = D_{2D}$ we recover the standard result for the one-dimensional diffusion equation with a non-time-dependent diffusion coefficient, i.e., $\sigma^2(t) = 2 D_{3D} t$ [1]. Essentially, $\sigma^2(t)$ represents a mean squared displacement of the polymer center of mass for polymers with time-dependent diffusion coefficients.

An expression for δ, the probability for a polymer to traverse (diffuse) forward in the ratchet, can now be obtained. To jump forward the polymer must diffuse a distance r_{eff} equal to the shortest dimension of the ratchet. The probability to do so is then obtained by integrating $P(x, t = t_{off})$ from $x = r_{eff}$ to $x = \infty$,

$$\delta = \int_{r_{eff}}^{\infty} P(x, t_{off}) dx = \frac{1}{2} \operatorname{erfc}\left[\left(\frac{1}{2} \frac{r_{eff}^2}{\sigma^2(t_{off})}\right)^{1/2}\right], \tag{22}$$

where erfc[ ] is the complementary error function [23]. We can then rewrite the distance r_{eff}^2 as $\sigma^2(t_r) = r_{eff}^2$, which defines

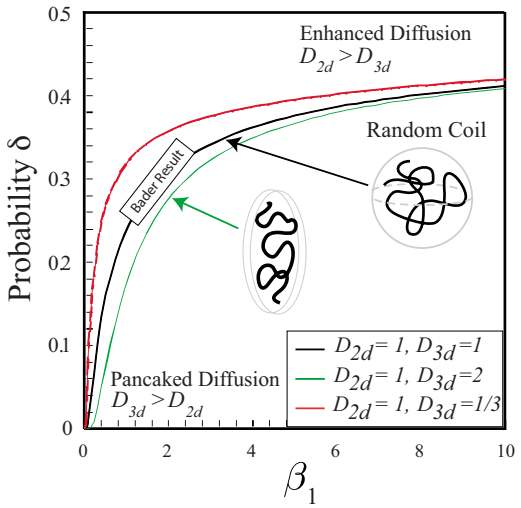

FIG. 6. (Color online) Probability δ for a polymer to diffuse forward in the ratchet as a function of the ratchet off time ($t_{\text{off}} = \beta_1 \tau_R$). The solid black line corresponds to the Bader result for an undeformed polymer $D(t) = D_{3\text{D}}$. The region above the black line corresponds to $D_{2\text{D}} > D_{3\text{D}}$, while the region below the black line corresponds $D_{3\text{D}} > D_{2\text{D}}$ and is the pancaked-polymer diffusion domain. Polymers in the pancaked diffusion regime are slowed and the associated value of δ is decreased.

t_r as the time required to diffuse the distance r_{eff}^2. The time t_r is obtained by inverting $\sigma^2(t_r) = r_{\text{eff}}^2$ for t_r, which gives

$$\frac{t_r}{\tau_R} = W_{\text{Lambert}}(-\Delta_D e^{-(\Delta_t + \Delta_D)}) + \Delta_t + \Delta_D,$$

$$\Delta_D = \left(1 - \frac{D_{2\text{D}}}{D_{3\text{D}}}\right) \quad \text{and} \quad \Delta_t = \frac{t_{\text{off}}^{\text{opt}}}{\tau_R}, \tag{23}$$

where $W_{\text{Lambert}}(x)$ is the inverse function of $f(x) = xe^x$ [23]. To reiterate, t_r is simply the time a polymer takes to diffuse forward one well. When there is no deformation $D_{2\text{D}} = D_{3\text{D}}$ and this time is simply the conventional estimate $t_r = t_{\text{off}}^{\text{opt}}$. We introduce the function W_{Lambert} here for simplicity of notation and to provide a closed form definition of t_r for the deformed polymers; actual values of t_r can be obtained numerically.

The resulting final probability δ is given by

$$\delta = \frac{1}{2}\,\text{erfc}\left[\left(\frac{1}{2}\frac{\sigma^2(t_r)}{\sigma^2(t_{\text{off}})}\right)^{1/2}\right] = \frac{1}{2}\,\text{erfc}\left[\left(\frac{1}{2}\frac{D_{3\text{D}}t_r - \tau_R(D_{3\text{D}} - D_{2\text{D}})(1 - e^{-t_r/\tau_R})}{D_{3\text{D}}t_{\text{off}} - \tau_R(D_{3\text{D}} - D_{2\text{D}})(1 - e^{-t_{\text{off}}/\tau_R})}\right)^{1/2}\right], \tag{24}$$

where t_r is given by Eq. (23). Eq. (24) is simplified by dividing the numerator and denominator by $D_{3\text{D}}\tau_R$. It is also useful to rewrite the time scales t_{off} and t_r in terms of the characteristic relaxation τ_R as $t_{\text{off}} = \beta_1 \tau_R$ and $t_r = \beta_0 \tau_R$. Doing this and simplifying the algebra, we obtain

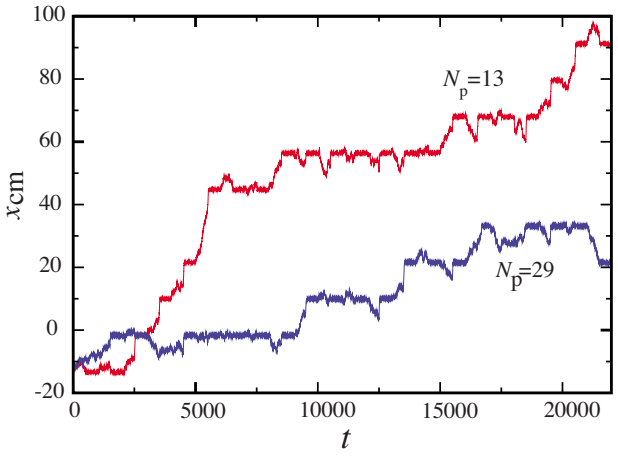

FIG. 7. (Color online) Typical trajectory of two different polymers with $N_p = 13$ and 29, for $t_{\text{off}} = t_{\text{on}} = 500$. The trajectories illustrate that the polymers are indeed undergoing a net motion which changes as a function of N_p. The ratchet has a depth of $U_0 = 4$, a width of $L_R = 11.61\sigma$, and an asymmetry factor of $\alpha = 0.80$.

$$\delta = \frac{1}{2}\,\text{erfc}\left[\left(\frac{1}{2}\frac{\beta_0 - \Delta_D(1 - e^{-\beta_0})}{\beta_1 - \Delta_D(1 - e^{-\beta_1})}\right)^{1/2}\right]. \tag{25}$$

Equation (25) is the probability for a deformed polymer with initial diffusion coefficient $D_{2\text{D}}$ to diffuse one or more well(s) in the ratchet. Equation (25) has three parameters: β_0, β_1, and the ratio of the 2D and 3D diffusion coefficients ($D_{2\text{D}}/D_{3\text{D}}$). It should be noted that β_0 is calculated from Eq. (23). In the case where $\Delta_D = 0$ the polymer is not deformed and we recover the original result of Bader *et al.*, given by

$$\delta_{\text{Bader}} = \frac{1}{2}\,\text{erfc}\left[\left(\frac{1}{2}\frac{\beta_0}{\beta_1}\right)^{1/2}\right] = \frac{1}{2}\,\text{erfc}\left[\left(\frac{1}{2}\frac{t_{\text{off}}^{\text{opt}}}{t_{\text{off}}}\right)^{1/2}\right], \tag{26}$$

the only difference being that the time scales are written in terms of τ_R.

Figure 6 shows a plot of the probability δ for a polymer to move forward, for three regimes. The solid black line is that corresponding to $D_{2\text{D}} = D_{3\text{D}}$, i.e., an undeformed polymer (corresponding to the original Bader expression). The other two curves on Fig. 6 correspond to $D_{2\text{D}} < D_{3\text{D}}$ for a pancaked-shaped polymer and $D_{2\text{D}} > D_{3\text{D}}$ for the case where the pancaked-polymer diffusion coefficient is greater than the free diffusion coefficient. The latter case is one in which deformation enhances diffusion in the pancake-shaped state and is not of interest in our work. This figure demonstrates several key features of our model. First, the transition probability δ for a pancake-shaped polymer ($D_{3\text{D}} > D_{2\text{D}}$) is decreased for short off times (i.e., small β_1). The latter suggests that deformation can be used to modulate the behavior of polymers in ratchets. Moreover, since large chains relax more slowly than shorter chains this effect of deformation would enhance the separation capability of a ratchet by slowing the movement of larger polymers more than that of smaller polymers. This is one of the key results of our work.

B. MD simulations and inhibited diffusion

We now turn to the results from our MD simulations. Figure 7 shows two typical trajectories of the polymer center of mass, for $N_p=13$ and 29, with $L_R=11.61\sigma$, $U_0=4$, and an asymmetry parameter of $\alpha=0.80$, from our MD simulations (we do not carry out a systematic study of the transport properties here). As seen in Fig. 7, the ratchet is able to induce net motion in two polymers with different lengths ($N_p=13$ and 29). The trajectories indicate that the molecules are moving with different speeds and the ratchet could be used to separate them. We provide only a single set of trajectories here although it is possible to extend our calculations to examine transport in these systems (it is, however, very computationally time consuming).

To explore the functional form of Eq. (20) we have carried out a suite of MD simulations which examine a single polymer ($N_p=29$) in the presence of a deep ratcheting potential with $U_0=10$, ensuring a high degree of deformation during the on phase of the ratchet. The on and off times of the ratchet are $t_{\rm off}=500$ and $t_{\rm on}=500$, given in MD time units. Evidently, $t_{\rm on}$ is much larger than the time scale required for the chain to be driven to the ratchet minima. From the MD simulations $R_g\simeq 3.6$ and the relaxation time calculated from Eq. (15) is $\tau_R\simeq 180$. The on and off times are then much larger than the relaxation time τ_R. The value of $t_{\rm off}$ is also chosen so that the polymer will have relaxed during the off phase. By flashing the ratchet off and on many times we generate trajectories of the position of the polymer center of mass as a function of time after the ratchet has been switched off. We map all particle trajectories onto the unit cell and calculate $\langle\sigma^2(t)\rangle$ from the MD simulations for the polymer of center of mass as a function of time. Figure 8 shows the mean squared displacement for the polymer center of mass obtained from multiple cycles of the ratchet. The ratchet width is $L_{\rm R}=11.61\sigma > R_{\rm g}\simeq 3.6$.

Figure 8 also shows (square symbols) the mean squared displacement of a single polymer ($N_p=29$) which is freely diffusing, i.e., normal diffusion in the absence of a ratchet potential. The data labeled ratchet (with circles) are those for a polymer released from a ratchet, which was on for a sufficiently long time to localize the polymer to the ratchet. The data are averaged over many cycles of the ratchet.

By carrying out a linear regression [using $\sigma^2(t)=2D_{\rm 3D}^{\rm MD}t$] of the free chain data we obtained a free diffusion coefficient of $D_{\rm 3D}^{\rm MD}\simeq 0.008\,15$. In the case of the ratchet we fit the data with the expression $\sigma^2(t)=2D_{\rm 3D}^{\rm MD}t-\phi$ obtained from the large-$t\gg\tau_R$ limit of Eq. (20). The constant $\phi=2\tau_R(D_{\rm 3D}^{\rm MD}-D_{\rm 2D}^{\rm MD})$ and is simply the prefactor of the second term in Eq. (20). The calculated value is $\phi=1.437$. Using the values of $D_{\rm 3D}^{\rm MD}$ and ϕ, we fit the ratchet data over the entire range of t using $\sigma^2(t)=2D_{\rm 3D}^{\rm MD}t-\phi[1-\exp(-t/\tau_R)]$ (where τ_R was the only fitting parameter). The value of the relaxation time thus obtained is $\tau_R^{\rm MD}\simeq 140$. Using the values of ϕ, τ_R, and $D_{\rm 3D}^{\rm MD}$ we calculated a value of the pancaked-polymer diffusion coefficient of $D_{\rm 2D}^{\rm MD}=0.003\,05$ or 35% of $D_{\rm 3D}^{\rm MD}$. The calculated relaxation time from Eq. (15), $\tau_R\simeq 180$, agrees well with $\tau_R^{\rm MD}\simeq 140$. The fitted line for the ratchet data is shown in Fig. 8 and describes well the data from the MD simulations over the whole range of t.

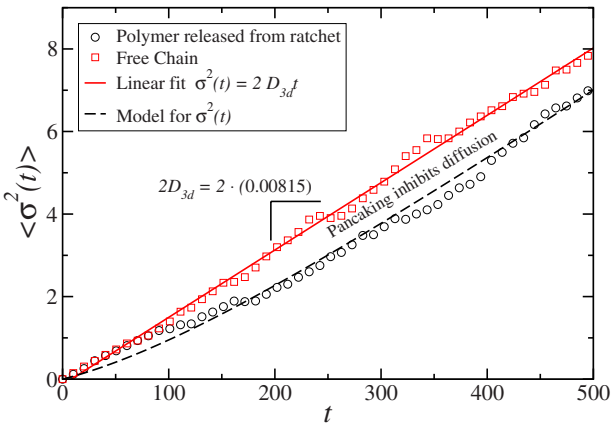

FIG. 8. (Color online) Averaged mean squared displacement $\langle\sigma^2(t)\rangle$ in the x direction versus time t for a free polymer and a polymer released from a ratchet from the MD simulations, with $N_p=29$, $\alpha=0.80$, and with a well depth of $U_0=10$. The free polymer (squares) undergoes normal diffusion (with $D_{\rm 3D}\simeq 0.008\,15$, obtained from a linear fit of the data). We can estimate the value of the relaxation time with a calculated value of $R_g^{\rm 3D}\simeq 3.6$ from the simulations: this yields an approximate value of $\tau_R^{\rm MD}\simeq 140$ calculated using Eq. (15). The polymer that is released from the ratchet is initially slowed and after a sufficient $t\simeq\tau_R$ returns to normal diffusive motion. This illustrates the effect of polymer pancaking on the reduction of the effective diffusion coefficient of a polymer released from a ratchet potential.

The MD simulation data illustrate and corroborate three important things. The first is that polymer diffusion is initially inhibited by the pancaking effect after release from the ratchet. The second point is that after some time ($t_{\rm off}\gg\tau_R$) the polymer resumes its normal diffusion. As the polymer relaxes over several multiples of its relaxation time, its diffusion coefficient returns to the 3D free diffusion value. Finally, there is an inherent lag time for the pancake-shaped polymers relative to free chains to diffuse the same mean squared distance $\sigma^2(t)$. For $t>\tau_R$, we can write $\sigma^2(t)\simeq 2D_{\rm 3D}t-2\tau_R(D_{\rm 3D}-D_{\rm 2D})$ and thus the time taken to diffuse $\sigma^2(t)$ is

$$t^*\simeq\frac{\sigma^2(t)+2\tau_R(D_{\rm 3D}-D_{\rm 2D})}{2D_{\rm 3D}}$$
$$\simeq\frac{\sigma^2(t)}{2D_{\rm 3D}}+\tau_R\Delta_D. \qquad (27)$$

Equation (27) is then simply the time taken for a free chain to diffuse $\sigma^2(t)/2D_{\rm 3D}$ plus a finite correction term given by $\tau_R\Delta_D$, with Δ_D given in Eq. (23). If we one use $D_{\rm 2D}=D_{\rm 3D}$ we recover the Bader *et al.* ratchet model [1], without corrections for deformation. In other words, by controlling Δ_D, i.e., the ratio of the pancaked-state diffusion coefficient relative to the free diffusion coefficient, it is possible to control this lag time and modulate the diffusion of polymers in a ratchet. The inhibited diffusion model and the diffusion occurring in the MD simulations agree well and the ratchet is slowed by the pancaking effect. This represents an operational tech-

nique and method to modulate polymer dynamics in a flashing ratchet.

V. CONCLUSIONS

We have presented an investigation of the effects of an applied asymmetric sawtooth potential on the properties of polymer chains. This potential both deforms (and compresses) the polymer chains and alters the Flory scaling of the polymers from free 3D polymers (ν_{3d}) to pancake-shaped 2D polymers (ν_{2d}). This compression modifies the polymer diffusion coefficient from the 3D free polymer diffusion coefficient, D_{3D}, to that of a 2D pancake-shaped polymer, D_{2D}. The initial diffusion of the polymer is then inhibited, resulting from the reduction in diffusion coefficient. We also illustrated that the width of the distribution describing the position of the center of mass of the polymer can be rather broad although we have not taken this into account in our modified ratchet theory.

We have presented a simple expression for the time-dependent diffusion coefficient $D(t)$ written in terms of the 2D diffusion coefficient D_{2D}, the 3D, diffusion coefficient D_{3D}, and the rotational relaxation time of the polymer τ_R. This expression quantitatively accounts for the observed inhibited diffusion of polymers released from ratchets and provides a second-order correction to existing polymer ratchet models. With our initial ansatz of a time-dependent diffusion coefficient we derived a modified Bader *et al.* ratchet model [1] which explicitly accounts for polymer deformation. We also provided a derivation of an exact expression for the polymer transition probability δ with a simple functional form. This transition probability directly takes into account the effect of deformation induced by the ratchet and in the limit of $D_{3D}=D_{2D}$ collapses to the original Bader *et al.* model.

Our modified ratchet model yields a transition probability which for short times ($t_{\text{off}}<\tau_R$) is less than that predicted by the Bader *et al.* model (for polymers starting from the pancaked state $D_{2D}<D_{3D}$). Although the Bader *et al.* model does give the correct first-order approximation to the problem it neglects second-order contributions from chain deformation. This is a direct result of the inhibited diffusion induced by the pancaking effect of the ratchet potential. It is worth noting that one may be able to generalize the Zimm model to arrive at an explicit expression for the time-dependent diffusion coefficient of a polymer chain confined to a ratchet potential although this is not something we pursue in this paper.

We demonstrated, using MD simulations, that the inhibited diffusion effect is directly observable in a ratchet. Moreover, this effect is presumed not to be present in Brownian dynamics simulations as a result of a non-conformation-dependent diffusion coefficient. We have shown that, by directly examining the diffusion of a polymer immediately after it is released from a ratchet potential and comparing it to a freely diffusing polymer, one can clearly see the effect of pancaking on diffusion. The result is that the pancaking effect slows the initial diffusion of the polymer chains and thus corroborates the proposed modified Bader *et al.* ratchet model. The data from the MD simulations illustrate the pancaking effect quite succinctly. Our model predicts that operational times for ratchets when defined in terms of the relaxation time of the polymer can be used to modulate polymer migration in a ratchet. The effect of pancaking can be used in an advantageous manner in experimental systems to control and optimize migration in ratchets. Since large chains will relax more slowly than smaller chains, this inhibited diffusion should enhance separation in ratchets.

ACKNOWLEDGMENTS

The authors would like to acknowledge the support of the Natural Sciences and Engineering Research Council of Canada (NSERC). The authors would like to thank Owen Hickey for useful discussions. M.K. would also like to thank the Ontario Ministry of Training, Colleges and Universities and the University of Ottawa for financial support. We also acknowledge the use of computational resources made available through both the High Performance Computing Virtual Laboratory (HPCVL) (www.hpcvl.org) and C3.ca.

[1] J. S. Bader, R. W. Hammond, S. A. Henck, M. W. Deem, G. A. McDermott, J. M. Bustillo, J. W. Simpson, G. T. Mulhern, and J. M. Rothberg, Proc. Natl. Acad. Sci. U.S.A. **96**, 13165 (1999).
[2] M. Bier, Contemp. Phys. **38**, 371 (1997).
[3] L. P. Faucheux, L. S. Bourdieu, P. D. Kaplan, and A. J. Libchaber, Phys. Rev. Lett. **74**, 1504 (1995).
[4] P. Reimann, Phys. Rep. **361**, 57 (2002).
[5] M. T. Downton, M. J. Zuckermann, E. M. Craig, M. Plischke, and H. Linke, Phys. Rev. E **73**, 011909 (2006).
[6] E. M. Craig, M. J. Zuckermann, and H. Linke, Phys. Rev. E **73**, 051106 (2006).
[7] J. C. T. Eijkel and A. van den Berg, Microfluid. Nanofluid. **1**, 249 (2005).
[8] J. Kauttonen, J. Merikoski, and O. Pulkkinen, Phys. Rev. E **77**, 061131 (2008).
[9] M. von Smoluchowski, Phys. Z. **17**, 557 (1916).
[10] R. P. Feynman, R. B. Leighton, and M. Sands, *The Feynman Lectures on Physics* (Addison-Wesley, Redwood City, CA, 1966).
[11] M. O. Magnasco and G. Stolovitzky, J. Stat. Phys. **93**, 615 (1998).
[12] R. D. Astumian and M. Bier, Phys. Rev. Lett. **72**, 1766 (1994).
[13] M. Kenward and G. W. Slater, Eur. Phys. J. E **14**, 55 (2004).
[14] M. Kenward and G. W. Slater, Eur. Phys. J. E **20**, 125 (2006).
[15] K. Kremer, G. S. Grest, and I. Carmesin, Phys. Rev. Lett. **61**, 566 (1988).
[16] K. Kremer and G. S. Grest, J. Chem. Phys. **92**, 5057 (1990).
[17] M. Allen and D. Tildesley, *Computer Simulation of Liquids* (Clarendon Press, Oxford, 1987).

[18] G. Besold, I. Vattulainen, M. Karttunen, and J. M. Polson, Phys. Rev. E **62**, R7611 (2000).
[19] I. Vattulainen, M. Karttunen, G. Besold, and J. M. Polson, J. Chem. Phys. **116**, 3967 (2002).
[20] I. Teraoka, *Polymer Solutions* (Wiley, New York, 2002).
[21] M. Doi and S. F. Edwards, *The Theory of Polymer Dynamics* (Oxford University Press, Oxford, 1986).
[22] H. Berg, *Random Walks in Biology* (Princeton University Press, Princeton, NJ, 1993).
[23] G. Arfken and H. Weber, *Mathematical Methods for Physicists* (Academic Press, New York, 1985).